BBAA VI International Colloquium on:
Bluff Bodies Aerodynamics & Applications
Milano, Italy, July, 20-24 2008

WIND TUNNEL TESTS ON TRAIN SCALED MODELS TO INVESTIGATE THE EFFECT OF INFRASTRUCTURE SCENARIO

Federico Cheli[*], Roberto Corradi[*], Daniele Rocchi[*], Gisella Tomasini[*] and Emilio Maestrini[†]

[*]Dipartimento di Ingegneria Meccanica
Politecnico di Milano, Campus Bovisa, Via La Masa 1, 20156 Milano, Italy
[†] Trenitalia, viale S. Lavagnini, Firenze
e-mail: federico.cheli@polimi.it, roberto.corradi@polimi.it, Daniele.rocchi@polimi.it, gisella.tomasini@polimi.it

Keywords: wind tunnel tests, cross wind, aerodynamic coefficients, infrastructure scenario, risk analysis

Abstract. *The cross wind risk analysis is today, within the European railway operators, one of the most important items related to the safety problem. In order to define the risk associated to the cross wind along a railway line, the effects of the infrastructure scenarios on the aerodynamic loads acting on a vehicle have to be investigated. A typical railway line is mainly characterized by two types of scenario: viaduct and embankment. In this work, the aerodynamic coefficients of the ETR500 train measured, through wind tunnel tests, for the standard TSI infrastructure scenarios (flat ground with and without ballast and rail and 6m-high embankment) and for a typical Italian viaduct are presented. Moreover, each infrastructure is characterized in terms of flow modification with and without the train model.*

1 INTRODUCTION

A new European Standard on cross wind effect on trains is under edition within the “Technical Specification for Interoperability” (TSI, Ref. [4]): it defines a methodology to evaluate the safety threshold for a rail vehicle subjected to cross wind action, in terms of CWC (Characteristic Wind Curve). The CWC represents the limiting wind speed that leads the vehicle to overcome a specific safety limit. The procedure, provided within the TSI consists in evaluating the trains CWC through time-domain simulations of the dynamic response of a vehicle subjected to turbulent cross-wind. The effect of turbulent wind is modeled through an equivalent impulsive input gust (Chinese hat). According to this methodology, the wind properties are fixed and the time histories of the aerodynamic forces depend only on the mean wind speed and on the train’s aerodynamic coefficients. These coefficients (and, as a consequence, the CWC) have to be determined starting from wind tunnel tests, for two infrastructure scenarios: the flat ground and a 6m-high standard embankment.

At the present state, from the rolling stock subsystem point of view, the TSI standard allows to consider a train as “interoperable” if its CWC satisfies specific limit reference values. From the infrastructure subsystem point of view, the infrastructure manager is required to identify all the parts of a line that can be exposed to severe winds, and to adopt the most appropriate countermeasures in order to ensure the operation safety. Nevertheless, in order to identify the most critical parts of a railway line it is necessary to combine the information of the wind characteristics with the information on the behaviour of a vehicle subjected to the cross wind, for the specific point along the line (Ref. [7] and [8]). In particular, in order to develop a methodology to perform a risk analysis of cross wind on high speed lines, it is important to understand the effect of the infrastructure scenarios on the aerodynamic coefficients.

A typical railway line is mainly characterized by two types of scenario: viaduct and embankment. In this work, the aerodynamic coefficients of the ETR500 train measured, through wind tunnel tests, for the standard TSI infrastructure scenarios (flat ground and 6m-high embankment) and for a typical Italian viaduct are presented and compared in order to understand the effects of infrastructure on aerodynamic loads.

2 WIND TUNNEL TESTS

Tests have been performed on different scenarios, with two scale-models of the ETR500 train:

- 1:10 model for tests on flat ground, with and without ballast and rail and on the 6-m high standard embankment (Figure 1);
- 1:20 model for tests with a typical Italian viaduct (Figure 2 and Figure 15).

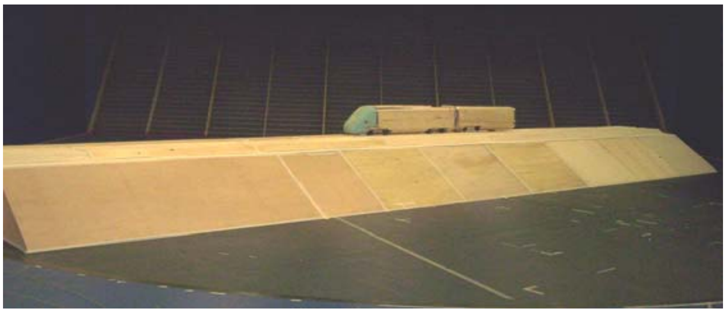

Figure 1. Experimental wind tunnel tests: 1:10 model of ETR500 on 6m high standard embankment.

Figure 2. Experimental wind tunnel tests: 1:20 model of ETR500 on a typical Italian viaduct.

All the tests have been performed in smooth flow conditions (Ref. [3]), with different wind angles of attack, from 0° (wind direction parallel and opposite to the train) to 90° (transversal wind). For each model scale, a specific experimental set up for the measurement of the aerodynamic forces on the power car and on the first trailer car has been designed.

2.1 Infrastructure scenario models

The flat ground corresponds to the condition of the train running on a flat terrain and it represents one of the reference configurations described by the TSI Standard Ref. [4]. In order to have a block profile for the mean wind speed, the flat ground scenario has been built using a circular wooden table (“splitter plane” thickness s=0.01 m, radius R=2.5m), positioned at a height of 0.3m from the wind tunnel floor (Figure 3). Figure 4 shows the vertical wind speed profile measured over the flat ground: the boundary layer thickness is very low and, over the range corresponding to the train extension, the wind speed variation is limited within the $\delta_{95\%}$, as required by TSI (Ref. [4]). The tests have been carried out on flat ground with rail, with and without ballast.

The 6 m high standard embankment (Figure 1) has been built in 1:10 scale according to the geometry reported in the TSI: with this infrastructure scenario, tests have been performed both for the train on the windward track and on the leeward track. Finally, the viaduct 1:20 scale model (Figure 15) has been designed according to the geometry of standard high speed Italian viaducts: the height of the viaduct is equal to 6 m at full scale.

Figure 3. Experimental wind tunnel tests: 1:10 scale model of ETR500 on flat ground with ballast and rail.

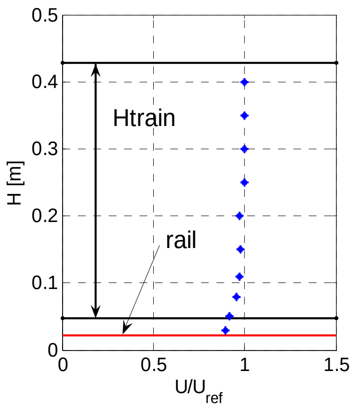

Figure 4. Flat ground without ballast: vertical profile of the mean wind speed.

2.2 Force measurement set up and reference system

In order to measure the aerodynamic forces acting on the 1:10 scale models of power car and of the first trailer car, a 6-components industrial dynamometric balance was adopted.

Figure 5 shows the connection system between balance and model. The dynamometric balance is connected to the train model by 4 beam elements in correspondence of the internal wheelsets. The model is suspended to the balance. The bogies and the wheelsets, that are geometrically similar to the corresponding real elements, are rigidly connected to the carbody: in this way, the aerodynamic forces that arise on all the external surfaces of the vehicle model are transferred, through the four connecting elements, only to the dynamometric balance.

The 1:20 scale model has been equipped with a 6-components internal dynamometric balance: this balance has been specifically designed for measuring the three aerodynamic forces and the three aerodynamic moments acting on the carbody, both in still and in moving model tests. As represented in Figure 6, the balance is composed by two horizontal plates, connected one to each other by means of seven miniaturized strain-gage load cells: four vertical dynamometers are positioned at the plates corners, two are positioned in the lateral direction (symmetrically with respect to the pitch axis), while a longitudinal load cell is put along the roll axis. Each load cell is linked to the plates through hinge-type constraints, in order to transmit the force only in the measurement direction. Since the upper plate is fixed to the carbody structure, while the lower one is connected to the bogies through elastic suspension elements, the balance measures the forces acting on all the carbody external surfaces.

The reference system adopted for the definition of the aerodynamic forces is fixed to the carbody and its origin is coincident with the carbody centre, at track height, as represented in Figure 5: x is the longitudinal axis, in the running direction, z is the vertical axis, upward directed, and y is perpendicular to define a right handed coordinate system. According to the CEN standard (Ref. [4]), the non-dimensional coefficients are defined as follows:

$$C_{Fi} = \frac{F_i}{\frac{1}{2}\rho \overline{U^2} S} \qquad\qquad C_{Mi} = \frac{M_i}{\frac{1}{2}\rho \overline{U^2} Sh} \tag{1}$$

where F_i (i=x,y,z) are the aerodynamic force components in the train's reference system (Figure 5) and M_i (i=x,y,z) are the corresponding moments, evaluated at the track height, in correspondence of the point P (Figure 5). In equation (1), ρ is the air density, $\overline{U^2}$ is the mean square value of the wind speed, *h* is equal to 3m, and *S* is a standard reference surface which is equal to 10 m^2.

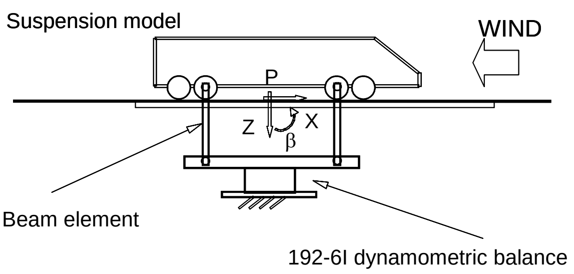

Figure 5. Scheme of connection between the external dynamometric balance and the 1:10 vehicle model.

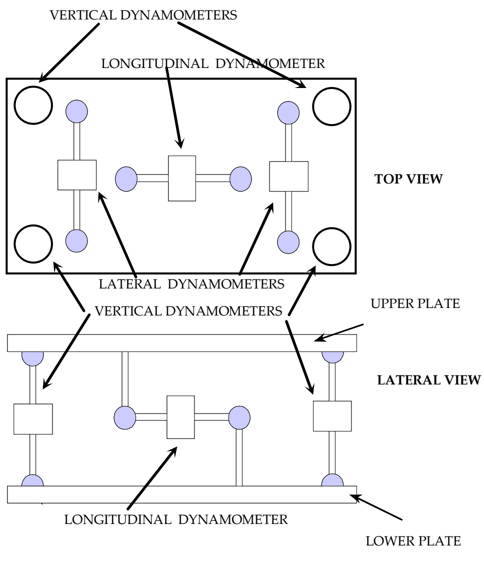

Figure 6. Internal dynamometric balance for 1:20 scale model for forces measurement: top view and lateral view.

3 AERODYNAMIC COEFFICIENTS FOR 1:10 SCALE ETR500 TRAIN MODEL

In this section, the aerodynamic coefficients measured on the 1:10 scale model of the ETR500 train are presented. Two infrastructure scenarios are considered, which are the same prescribed in the TSI standard: flat ground and 6m-high standard embankment. The results for both power car and first trailer car are reported.

Figure 7 shows the aerodynamic coefficients measured on the 1:10 scale model of the power and trailer car of the ETR500 train on flat ground scenario for different wind angles of attack.

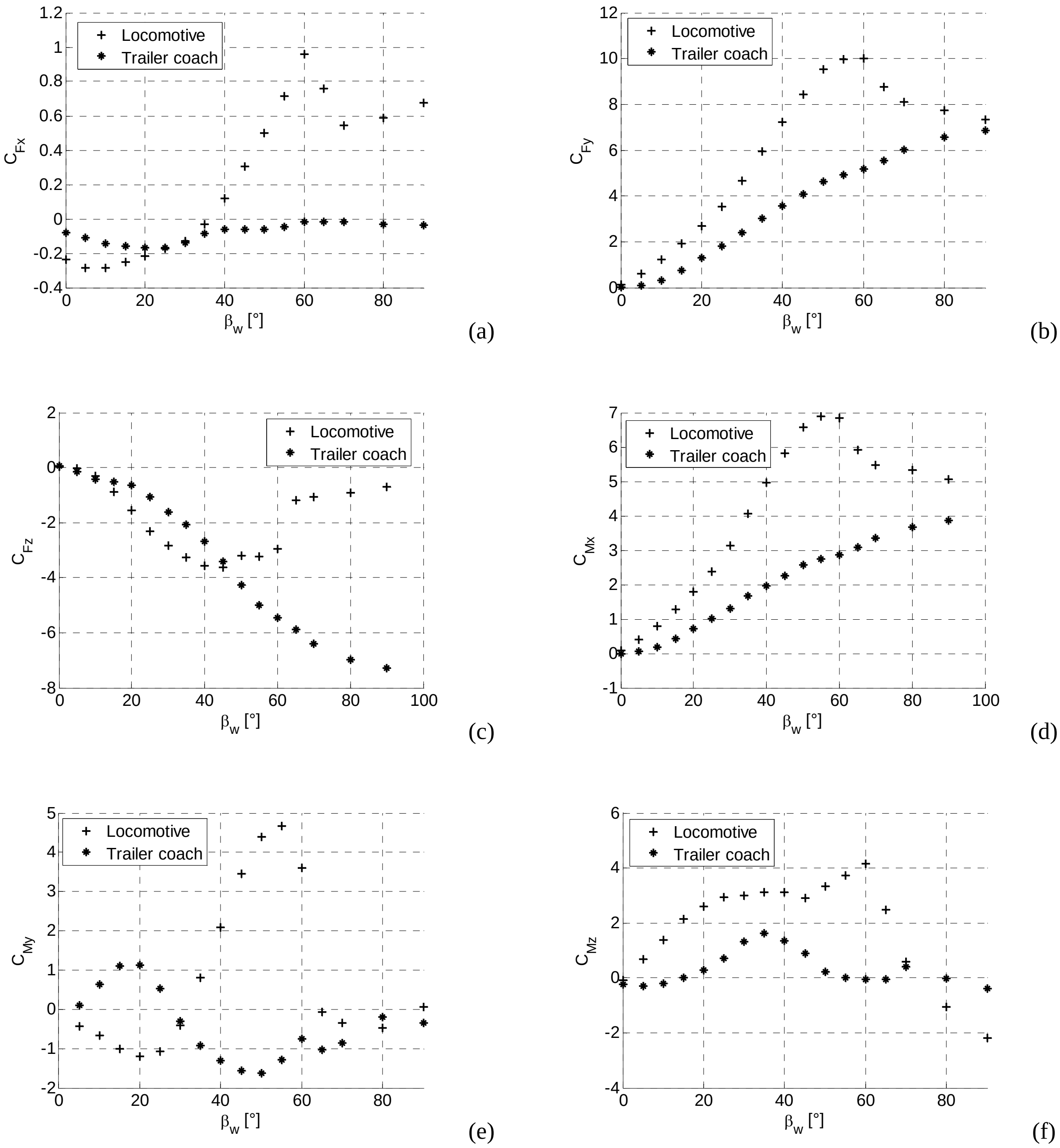

Figure 7. Aerodynamic force coefficients of ETR500 train, 1:10 scale model, flat ground: locomotive vs first trailer coach (CEN conventions).

It is possible to observe that the first vehicle shows, for all the coefficients, a maximum for angles between 55 and 60 degrees, while the second vehicle reaches its maximum, for the vertical force, the lateral force and the roll moment coefficient, at 90°. The coefficient trend with the angle of attack found for the locomotive is typical of all the leading vehicles of a convoy

(Ref. [1], [2], [3], [4], [5] and [6]) and it is due to a transition from slender to bluff body aerodynamic behaviour. Moreover, Figure 7 shows also that the first vehicle is characterized by a roll moment coefficient higher than the one of the second vehicle for all the angles of attack; on the other hand, the values of the vertical force coefficient of the power car are higher than those of the trailer car only in the range 10°-45°. As a consequence, the first vehicle is considered as the most critical in terms of risk of overturning and it is the only one that will be analysed in the risk analysis.

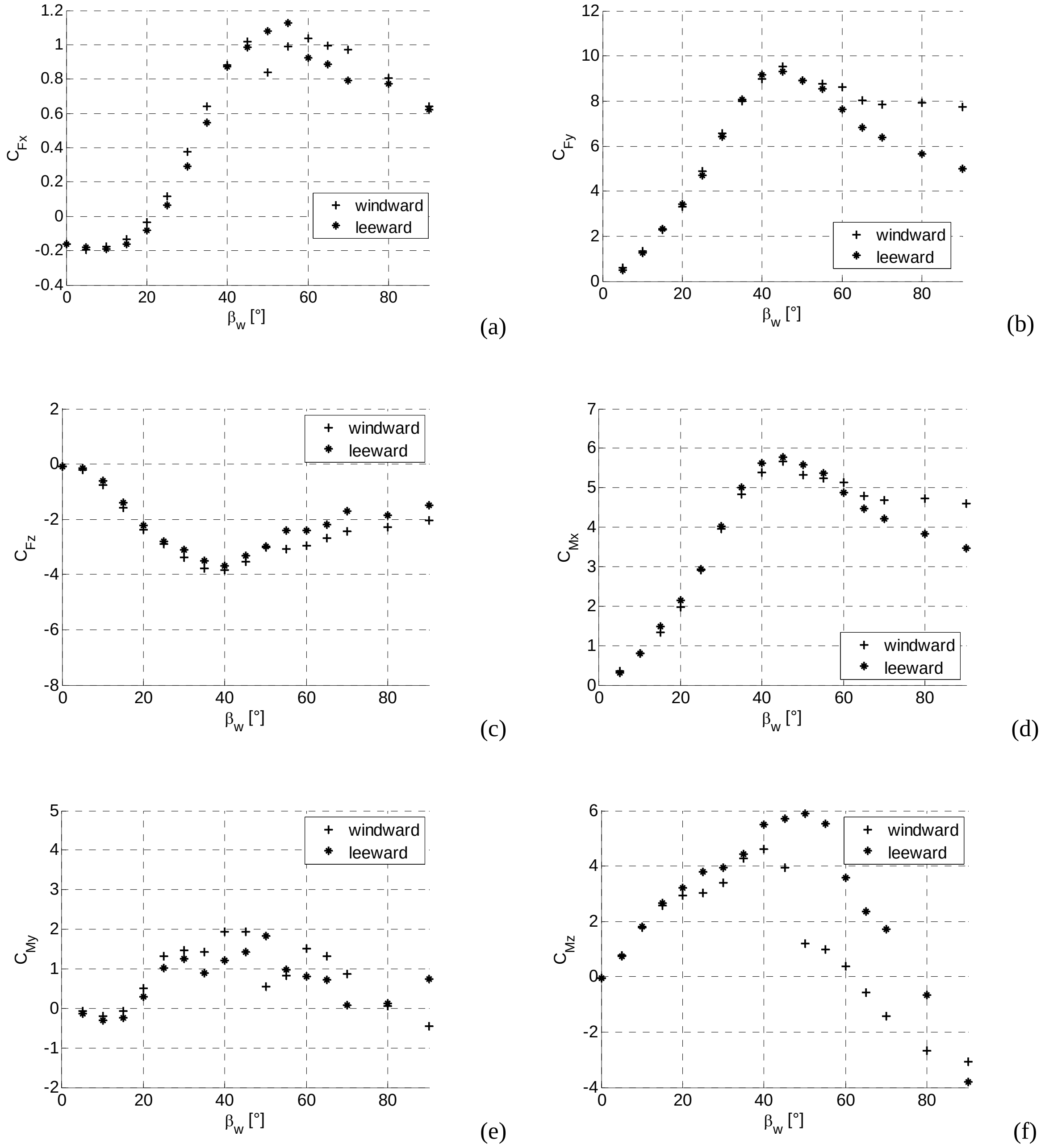

Figure 8. Aerodynamic force coefficients of ETR500, 1:10 scale model, 6m high standard embankment, locomotive: windward vs leeward side (CEN conventions).

The same aerodynamic coefficients for the first vehicle of the ETR500 train on a 6m-high embankment are shown in Figure 8, where a comparison between windward and leeward train's position is reported. It is possible to observe that the main differences between the two configurations arise, for all the coefficients, at high angles of attack, while at low angles all the coefficients do not seem to be significantly sensitive to the train position on the embankment.

4 INFRASTRUCTURE SCENARIO EFFECTS

It is well known that the infrastructure's geometry influences the aerodynamic response of a rail vehicle (Ref. [2], [3] and [6]). In this section, the 6m-high standard embankment and a typical railway viaduct have been considered and compared, in terms of aerodynamic coefficients, with the flat ground configuration and the effect of the scenario on wind speed will be analysed.

4.1 Embankment

In order to investigate the flow modification induced by the infrastructure scenarios some preliminary tests have been performed without train model but with a pitot tube positioned in correspondence of the train position: in these tests the wind speed is measured both in free stream (far away upwind the scenario) and in a point 0.2m high (that corresponds to 2m in real scale) over the top of the rail.

Figure 9 shows the experimental set up adopted for the tests while Figure 10 shows the trend of the ratio between the wind speed measured by the pitot tube on the 6m high standard embankment and the wind tunnel speed measured in free stream. It is possible to observe that the acceleration due to the embankment is increasing with the angle of attack: the ratio goes from 1, in correspondence of wind parallel to the scenario to about 1.3, for perpendicular wind.

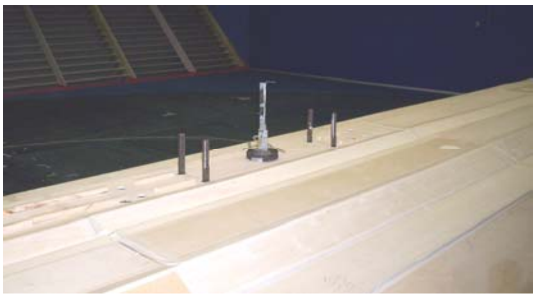

Figure 9. Embankment characterization tests: pitot tube over the embankment model (1:10 scale).

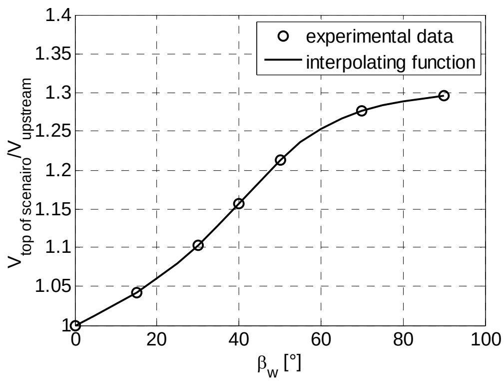

Figure 10. Embankment characterization tests: ratio between wind speed measured over the embankment and in free stream.

Figure 11 shows a comparison of the roll moment and the vertical force coefficients measured on the 1:10 scale model of ETR500 power car, between the 6m-high embankment scenario (windward) and the flat ground configuration without ballast. In particular, the aerodynamic coefficients measured on the windward side of the embankment have been computed by making reference to the incoming wind speed measured in two different positions: marker * refers to the coefficients evaluated using the wind speed of undisturbed flow (free stream), while marker *x* corresponds to the coefficients calculated adopting the wind speed measured over the embankment, (without the train, in correspondence of the train position).

This second procedure is adopted to account for the speed up effect associated to the infrastructure scenario.

The data reported in Figure 11 confirm the indisputable effect of the scenario on a train's aerodynamic behaviour. Considering the wind speed measured in free stream, the roll moment coefficient for train on embankment differs from the flat ground one, also for small angles of attack. In particular, the previous one is higher up to 40° and lower for larger angles of attack. If the roll moment coefficient for the embankment scenario is evaluated on the basis of the wind speed measured over the track, at low yaw angles (up to 35°), the coefficient itself is very close to the corresponding coefficient measured on flat ground. This demonstrates that, at low angles, the gap in the roll moment coefficient between flat ground and embankment can be substantially ascribed to the speed up effect associated to the geometry of the embankment. The practical outcome of this experimental result is that the flat ground coefficients can be used also for the embankment scenario provided that the accelerated wind speed on top of the embankment is adopted as the reference one for the aerodynamic loads computation. Effective formulas are proposed in literature to account for this speed up effect (Ref. [2]).

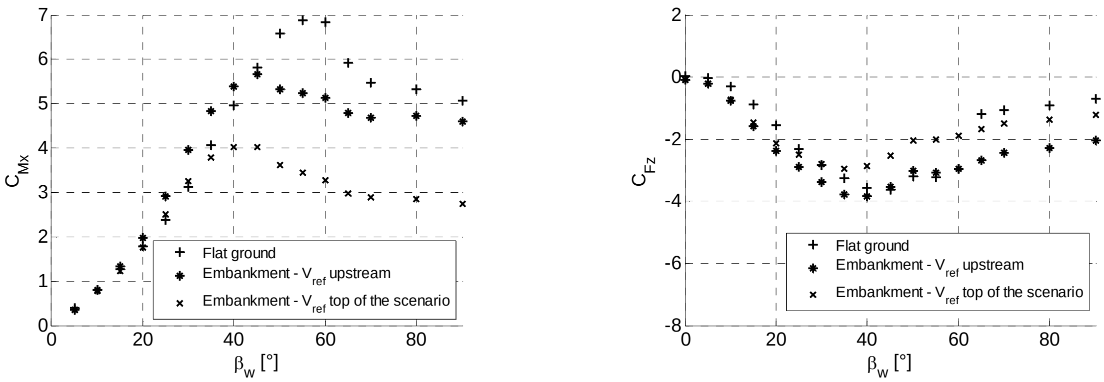

Figure 11. ETR500 1:10 model, trailer: roll moment coefficients (on the left) and vertical force coefficients (on the right) on embankment, windward, with reference speed upstream (+) and at the top of scenario (*), and on flat ground (x).

Looking again at Figure 11, if we consider large angles of attack, the aerodynamic behaviour of the train is so influenced by the combined geometry of the complete system (train and embankment) that the physical phenomenon can not be simply reduced to a corrective coefficient related to the speed up effect, but the actual system geometry must be taken into account. In any case, it must be remembered that, when dealing with high speed trains, the train itself generally experiences wind angles of attack smaller than 30°, also for limiting wind speeds. As a consequence, the correction proposed for small angles of attack can be considered a useful mean to perform risk analysis calculations of specific embankment scenarios, starting from flat ground coefficients measured in wind tunnel. On the other hand, from Figure 11 it is possible to see that, up to 30°, the vertical force coefficient C_{Fz} measured on flat ground is lower than that measured on embankment, also considering the wind speed on the top of the scenario. It is the authors' opinion that, in this case, the discrepancy between the two results is due to the different boundary conditions in the underbody zone.

In Figure 12 the same comparison shown in Figure 11 is proposed for the aerodynamic coefficients, C_{Mx} and C_{Fz}, measured on the leeward side of the 6m-high embankment scenario and evaluated with both the reference wind speeds: since the aerodynamic coefficients for the windward and the leeward configurations are not significantly different, similar observations can be drawn.

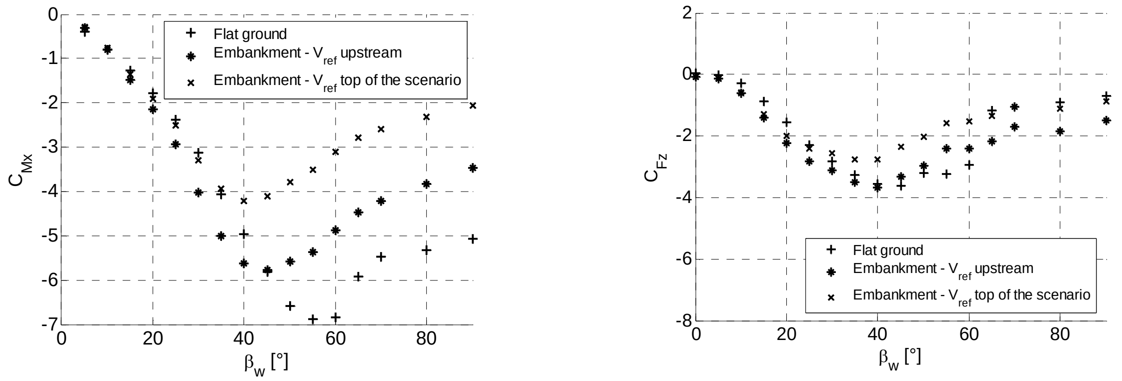

Figure 12. ETR500 1:10 model, trailer: roll moment coefficients (on the left) and vertical force coefficients (on the right) on embankment, leeward, with reference speed upstream (+) and at the top of scenario (*), and on flat ground (x).

The same analysis has been performed also on an other high speed trains with the same scenarios. Figure 13 shows the roll moment and the vertical force coefficients measured on a 1:10 scale model of the power car of an high speed train: also in this case the aerodynamic coefficients measured on the standard 6m-high embankment have been calculated by using, as reference speed, both the upstream speed and the velocity measured on the top of the embankment.

It is possible to see that, also for this train, the roll moment coefficient evaluated by making reference to the wind speed at the top of the scenario is almost equivalent to the corresponding flat ground coefficients but, in this case, this behaviour is verified only for a smaller range of angles of attack, from 0° up to 20°-25°. In the same range of angles of attack, the vertical force coefficient measured on the embankment by considering the wind velocity at top of the scenario get near to the corresponding coefficients measured on the flat ground and, for higher angles of attack (between 30° to 45°) the gap between the two coefficients is almost completely filled.

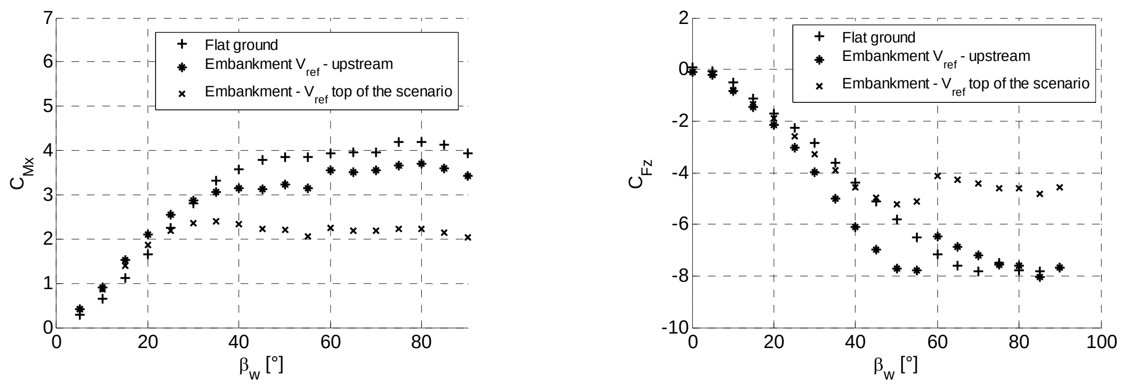

Figure 13. High speed train, 1:10 model, trailer: roll moment coefficients (on the left) and vertical force coefficients (on the right) on embankment, windward, with reference speed upstream (+) and at the top of scenario (*), and on flat ground (x).

From these observations, it is possible to conclude that the flat ground coefficients are equivalent, in terms of roll moment, to the ones measured on the embankment and calculated by

adopting, as reference velocity, the wind speed measured on the track, for low angles of attack but the range of angles where this assumption if verified depends on the train aerodynamics.
The correction associated to the acceleration of flow can not completely fill the gap between embankment and flat ground results for the vertical force coefficient because this coefficient is particularly influenced by the boundary conditions in the underbody zone.
Figure 14 shows a comparison between the 6m-high embankment scenario (windward) and the flat ground configuration with ballast and rail.
It is possible to observe that the roll moment coefficients measured with the flat ground with ballast and rail are not significantly different from what is measured on flat ground without ballast: as a consequence, the remarks undertaken for the case of flat ground without ballast relative to the roll moment coefficient can be extended also to the case of flat ground with ballast and rail. Looking again at Figure 14, when considering the vertical force coefficient, the coefficients measured with the embankment, evaluated by making reference to the upstream wind velocity, are in good agreement with the corresponding coefficient relative to the flat ground with ballast and rail up to about 30°-35° angle of attack. The direct consequences of this result are that the speed up effect associated to the embankment seem not to have significant influence on the vertical force coefficient and the differences between vertical force coefficients measured in different scenarios (see Figure 11) are mainly due to the boundary conditions in the underbody zone that are similar between embankment and ballast and rail.

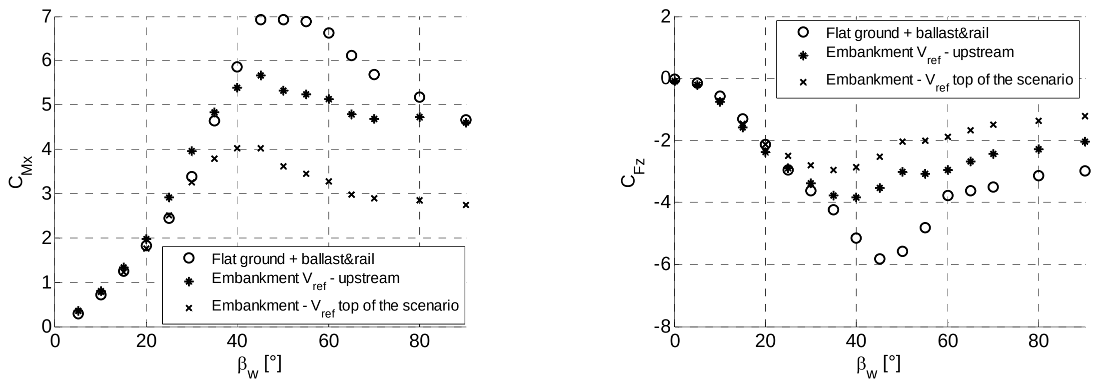

Figure 14. ETR500 1:10 model, coach: roll moment coefficients (on the left) and vertical force coefficients (on the right) on embankment, windward, with reference speed upstream (+) and at the top of scenario (*), and on flat ground+ballast&rail (x).

4.2 Viaduct

Also for the viaduct scenario, tests have been performed without train model in order to evaluate the effect of the viaduct 1:20 scale model on the flow field. As represented in Figure 15, the experimental set up is composed by a cobra probe, positioned at a height of 0.2m over the top of the rail (that correspond to 4m in real scale): this instrument allows the measurement of the three components of the wind velocity. Moreover, during these tests, the wind speed is measured by a pitot tube set away upwind the viaduct.

Tests have been performed with and without a nose positioned in front of the viaduct in order to highlight the effects of the finite boundary of the viaduct model on the flow field.

Figure 16 shows the ratio between the horizontal wind velocity measured by the cobra probe at top of the scenario and the same component measured upstream by the pitot tube for the viaduct with and without nose (Figure 15), as a function of the angle of attack.

From these experimental results it is clear that, except at β_W=0° and β_W=5° (where the effects of the finite boundary of the viaduct model are significant), the wind speed on the top of the viaduct is equivalent to that measured upstream up to β_W=35°. Moreover, we can observe that there are not relevant variations between the speed measured over the top of the scenario with and without the nose.

Finally, Figure 17 shows the ratio between the vertical component of the wind velocity measured by both the cobra probe at top of the scenario and the same component measured upstream for the viaduct with the nose. The vertical component remains lower than 5% of the upstream wind velocity at almost all the angles of attack.

In conclusion, for the considered viaduct and up to about 35°-40°, using the wind speed measured at an height equivalent, in real scale, to 4m over the top of the scenario, the effects on the flow field associated to the viaduct scenario can be considered negligible.

Figure 15. Viaduct with nose, characterization tests: cobra probe over the viaduct model (1:20 scale).

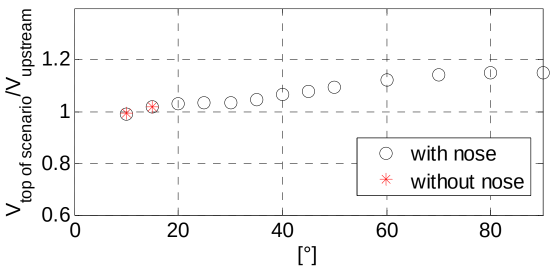

Figure 16. Viaduct, horizontal component wind speed: viaduct model with nose (black points) and without nose (red points).

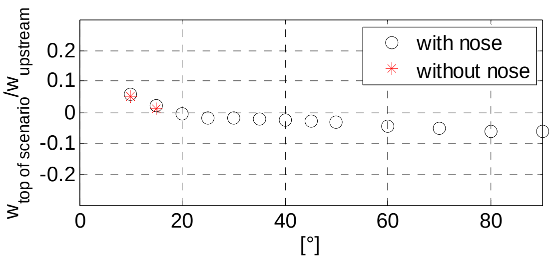

Figure 17. Viaduct with nose, vertical component wind speed: ratio between wind speed measured over the embankment and upstream.

Figure 18 shows the roll moment and the vertical force coefficients measured on the 1:20 scale model of the power car of the ETR500 train on viaduct, in windward and leeward position, in comparison with the corresponding coefficients measured on the 1:10 scale model of the same vehicle on flat ground without ballast. The coefficients of the viaduct configuration have been calculated by adopting, as reference wind velocity, the upstream speed. It is possible to observe that, up to α=40°, the roll moment coefficients measured with the flat ground is in a good agreement with the highest between the coefficients measured, at each angle, in windward and leeward configurations on viaduct. On the other hand, for the vertical force coefficients, the gap between the three analysed configurations is more important: for angles of attack up to 35°, the coefficients measured with the flat ground are more critical than what is measured with both the configurations on viaduct.

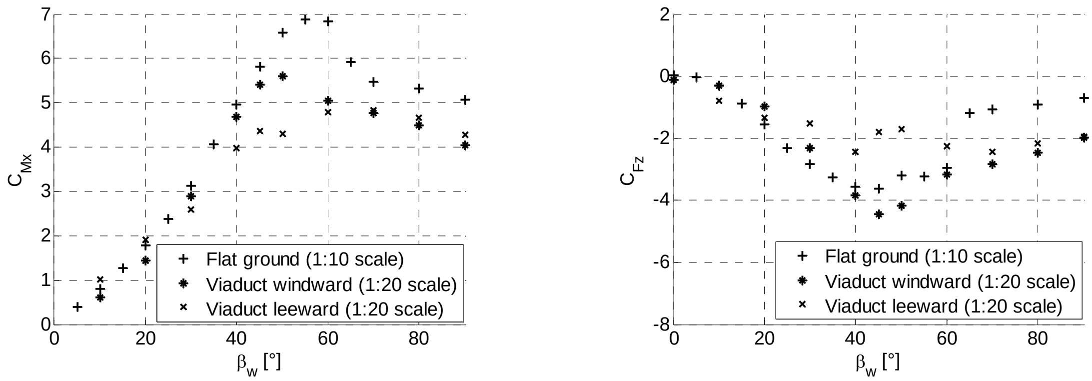

Figure 18. ETR500 1:10 model, trailer: roll moment coefficients (on the left) and vertical force coefficients (on the right) on flat ground (+) and on viaduct, windward (*) and leeward (x).

5 CONCLUSIONS

The aerodynamic coefficients of the ETR500 train measured, through wind tunnel tests, for the standard TSI infrastructure scenarios (flat ground with and without ballast and 6m-high embankment) have been shown.

Moreover, in order to understand the effect of the scenarios on the aerodynamic coefficients, two typical infrastructure scenarios (embankment and viaduct) of a railway line have been characterized through wind tunnel tests with and without the vehicle model.

From the experimental results carried out on the embankment with different train models, it is possible to conclude that the roll moment coefficient is affected by the speed up associated to the scenario. At low angles of attack, if the coefficient is defined by adopting, as reference velocity, the wind speed measured over the track, it is equivalent to the one measured on the flat ground. On the contrary, also from the tests carried out on flat ground with ballast and rail, it has been highlighted that the vertical force coefficient is not significantly influenced by the flow acceleration but it is mainly influenced by the boundary conditions in the underbody zone: in fact, the lift coefficient measured with the embankment, at low angles of attack is very similar to that found on flat ground with ballast and rail.

Finally, the tests performed with the typical Italian viaduct without the train model have shown that, up to about 40°, the effects on the flow field associated to the scenario can be considered negligible. The corresponding roll moment coefficient, in the same range of angles of attack, is not so different from that measured on flat ground.

ACKNOWLEDGEMENTS

The research has been developed with the financial support of TRENITALIA Gruppo FS, which also provided the physical train models for the wind tunnel experimental tests.

REFERENCES

[1] C.J. Baker. Ground vehicles in high cross winds Part 1 Steady Aerodynamic forces. *Journal of Wind Engineering and Industrial Aerodynamics,* **5**, 69-90, 1991.

[2] C.J. Baker. The wind tunnel determination of crosswind forces and moments on a high speed train. *Numerical Fluid Mechanics*, Springer-Verlag Berlin, **79**, 46-60, 2002.

[3] Bocciolone M., Cheli F., Corradi R., Muggiasca S., Gisella Tomasini. Crosswind action on rail vehicles: wind tunnel experimental analyses. *Journal of Wind Engineering and Industrial Aerodynamics*, **96**, 584-610, 2008.

[4] Technical Specification for Interoperability. Draft Revised HS RST TSI.

[5] C.J. Baker, J. Jones, F. Lopez-Calleja, J. Munday. Measurements of the cross wind forces on trains. *Journal of Wind Engineering and Industrial Aerodynamics*, **92**, 547-563, 2004.

[6] M. Bocciolone, F. Cheli, R. Corradi, G. Diana, G. Tomasini. Wind tunnel tests for the identification of the aerodynamic forces on rail vehicles. Proceedings of 11th ICWE, Lubbock, Texas, June 2-5, 2003.

[7] G. Diana, M. Burlando, F. Cheli, A. Freda, C. F. Ratto, D. Rocchi, G. Solari, M. Testa, G. Tomasini. A new methodology to perform the risk analysis of cross wind on high speed lines. Proceedings of 8th WCRR, Seul, Korea, May 18-22, 2008.

[8] F. Cheli, F. Ripamonti, D. Rocchi, G. Tomasini, M. Testa. Risk analysis of cross wind on HS/HC Rome-Naples railway line. Proceedings of the BBAA VI, Milano, Italy, July 20-24, 2008.